N_2O decomposition over Fe/ZSM-5: effect of high-temperature calcination and steaming

Q. Zhu [a], B.L. Mojet [a,†], R.A.J. Janssen [b], E.J.M. Hensen [a,*], J. van Grondelle [a], P.C.M.M. Magusin [a], and R.A. van Santen [a]

[a] *Schuit Institute of Catalysis, Laboratory of Inorganic Chemistry and Catalysis, Eindhoven University of Technology, P.O. Box 513, 5600 MB, Eindhoven, The Netherlands*

[b] *Laboratory of Macromolecular and Organic Chemistry, Eindhoven University of Technology, P.O. Box 513, 5600 MB, Eindhoven, The Netherlands*

Received 22 January 2002; accepted 11 March 2002

N_2O decomposition over Fe/ZSM-5 made by the sublimation method was investigated. Further calcination or steaming treatment (700 °C) increased the decomposition rate of N_2O. FTIR showed that such treatments lead to the disappearance of Brønsted acid sites. The various catalysts have different apparent activation energies, confirming the presence of different active Fe species. The observation that after high-temperature calcination a higher activity is obtained while no dealumination occurs indicates a mechanism where neutral Fe oxide clusters occluded in the zeolite micropores react at high temperature with the zeolite protons to form $[FeO]^+$-like species.

KEY WORDS: Fe/ZSM-5; N_2O decomposition; apparent activation energy; pre-exponential factor.

1. Introduction

Transition metals occluded in zeolites provide a wide variety of catalytic functionalities [1]. Among the ion-exchanged zeolites, over-exchanged Fe/ZSM-5 has attracted much attention recently because it is considered to be one of the most promising candidates for selective catalytic reduction (SCR) of nitrogen oxides such as those present in lean-burn engines [2–5]. Therefore, it is a matter of considerable academic and industrial interest to know the nature of the over-exchanged Fe/ZSM-5. Feng and Hall [2,3] first reported an unusual way to prepare such over-exchanged Fe/ZSM-5, suggesting that $Fe(OH)^+$ replaces the sodium ion, thus acting as an active site in the SCR of NO_x. Sachtler and co-workers [4–8] later reported an easy-to-prepare over-exchanged Fe/ZSM-5 by the sublimation method and a binuclear cluster $[HO{-}Fe{-}O{-}Fe{-}OH]^+$ was proposed to be the active site. A binuclear Fe cluster was also proposed by Panov and co-workers [9–14], partly inspired by the binuclear Fe center in the methane monooxygenase (MMO), as the active site in benzene hydroxylation to phenol by N_2O over Fe/ZSM-5 catalyst, although this catalyst has been prepared differently and has lower Fe loading. Remarkably, Marturano *et al.* [15] and Battiston *et al.* [16] independently reported the presence of diferric oxo/hydroxo-bridged clusters using EXAFS data, although the application of such a technique is debated for this heterogeneous system [17]. On the other hand, Joyner and Stockenhuber [18] concluded from using EXAFS that the small oxygen-containing nanoclusters, maybe Fe_4O_4, in Fe/ZSM-5 are more active (per iron atom) in the SCR reaction than the isolated cations. However, it was reported that the oxidation state of Fe depends also on the Fe content in the zeolites, indicating the complexity of the Fe/ZSM-5 system [19].

The over-exchanged Fe/ZSM-5 prepared by sublimation is also an effective catalyst for N_2O decomposition [20–22]. Interestingly, the decomposition of N_2O is a particularly simple reaction in which N_2O acts as both the oxidizing and reducing agent, rendering one of the most straightforward chemical tools available to study the redox system. Furthermore, recent agreements by most countries to reduce the greenhouse gas emissions, in which N_2O contributes 9% of the overall greenhouse effect, highlights the necessity to control the nitrous oxide release in which the catalytic decomposition is the easiest way.

In the present work, N_2O decomposition is used as a probe reaction to elucidate the nature of active sites in over-exchanged Fe/ZSM-5 prepared by the sublimation method. Based on both detailed kinetic study and spectroscopic characterization methods, we will propose a mechanism related to the transformation of different Fe species inside the zeolites during high-temperature calcination, unveiling their roles as possible active sites in the N_2O decomposition.

* To whom correspondence should be addressed.
† Current address: Department of Chemical Technology, Catalytic Processes and Materials, University of Twente, P.O. Box 217, 7500 AE, Enschede, The Netherlands.
E-mail: E.J.M.Hensen@tue.nl

1011-372X/02/0800-0205/0

2. Experimental

2.1. Catalyst preparation

2.1.1. Original Fe/ZSM-5

The initial parent NH_4ZSM-5 zeolites with different Si/Al ratio (20 or 30) were kindly provided by Akzo-Nobel. Anhydrous $FeCl_3$ reagent grade 99.9% was obtained from Aldrich. HZSM-5 was prepared by calcining NH_4ZSM-5 at 550 °C in a flow of pure O_2. From these two batches of HZSM-5, Fe/ZSM-5 was prepared by the sublimation method described elsewhere [4,5]. The temperature of $FeCl_3$ (boiling point 315 °C) was 300 °C and the temperature of HZSM-5 was 320 °C. Subsequently, the sample was washed in 2500 ml deionized water twice, stirring for 1 h each time. After drying in an oven at 110 °C overnight, 1 g Fe/ZSM-5 was calcined at 550 °C in a flow of 20% O_2/He (200 ml/min) for 2 h. Since we followed the original preparation procedure [4,5], the sample is designated as "original Fe/ZSM-5".

2.1.2. High-temperature calcined or steamed Fe/ZSM-5

Further treatment of the original catalyst was carried out at relatively high temperature. (a) 0.2 g original Fe/ZSM-5 was calcined in a flow of 20% O_2/He (200 ml/min) at 700 °C for 3 h. The catalyst is referred to as high-temperature calcined Fe/ZSM-5. (b) 0.2 g original catalyst was steamed in a flow of 20% O_2/He (200 ml/min) with 10% water vapor at 700 °C for 3 h. The catalyst is denoted as steamed Fe/ZSM-5.

2.2. Reaction studies

Reaction data were collected using a plug-flow reactor and a well-calibrated online quadrupole mass spectrometer as the analyzing equipment. Typically, 3500 ppm N_2O/He at 32 ml/min was used as feed gas. A bypass allowed the measurement of both feed gas and outlet products, using $m/e = 44$ for N_2O, $m/e = 28$ for N_2, $m/e = 32$ for O_2 and $m/e = 4$ for He. Additionally, $m/e = 30$ for NO and $m/e = 46$ for NO_2 were applied and all the fragmentations were fully considered. An amount of 0.04 g Fe/ZSM-5 (sieve fraction 125–425 μm) was diluted with SiC to fulfill plug-flow requirements. The catalyst bed was located in the middle part of a quartz tube reactor with inner diameter of 0.4 cm and was held in place with quartz wool. The Fe/ZSM-5 volume was approximately 0.08 cm^3 while the catalyst bed was ~2 cm long by the dilution with SiC. All the catalysts were pretreated in a flow of 20% O_2/He (200 ml/min) at 550 °C for 1 h prior to reaction. After some initial deactivation, a steady state is achieved within 1 h.

2.3. Characterization

2.3.1. Elemental analysis

The composition of the prepared samples (Si, Al and Fe) was carried out by the ICP-OCES technique after the Fe/ZSM-5 sample was dissolved in an acid mixture (HF and HNO_3).

2.3.2. Infrared spectroscopy

Infrared spectra of self-supporting 10 mg catalyst wafers were recorded at room temperature on a Bruker IFS113 Fourier transform IR spectrometer with DTGS detector at a resolution of 4 cm^{-1}. Prior to IR measurement, the catalyst was pretreated *in situ* at 500 °C for 1 h *in vacuo* (pressure lowered to 10^{-6} mbar). Normalization of the overtones of lattice vibration (1870–1950 cm^{-1}) was applied to achieve the quantification of Brønsted acid sites.

2.3.3. NMR

Solid-state ^{27}Al magic-angle spinning NMR spectra were obtained on a Bruker Ultrashield 500 spectrometer at a magnetic field of 11.7 T, equipped with a 4 mm MAS probe head. The Al resonance frequency at this field was 130 MHz. The sample rotation speed was 12.5 kHz. The ^{27}Al chemical shifts were referenced to a saturated $Al(NO_3)_3$ solution.

2.3.4. ESR

ESR experiments were carried out with a Bruker ESP 300E spectrometer, operating with an X-band standard cavity (9.44 GHz), an ER 035 M NMR Gauss meter, and an HP 5350B frequency counter. A 100 kHz modulation of 5 G and 2 mW microwave power were used to record the spectra. The field axis in figure 7 was corrected for the variations in frequency in different spectra. The spectra were recorded at 10 K with the use of an Oxford continuous flow cryostat and variable temperature unit.

3. Results

3.1. Elemental analysis

Table 1 shows the elemental composition of the original catalysts, the number in parentheses indicating the approximate Si/Al ratio of the catalysts. No change in elemental content is found after further treatment (700 °C calcination or steaming) of the original Fe/ZSM-5. The relatively low Al content Fe/ZSM-5(30) has a similar Fe content to Fe/ZSM-5(20), leading to

Table 1
Elemental analysis for catalysts prepared

	Si/Al	Al content (wt%)	Fe content (wt%)	Fe/Al
Fe/ZSM-5(20)	19.4	1.79	3.60	0.97
Fe/ZSM-5(30)	27.5	1.34	3.62	1.30

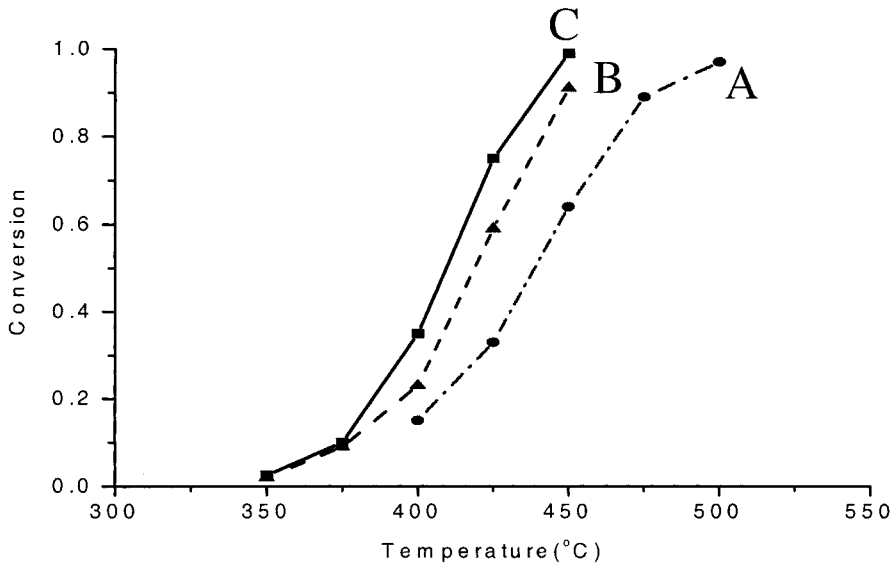

Figure 1. N_2O decomposition on Fe/ZSM-5(20). Feed concentration: 3500 ppm GHSV = 24 000 h^{-1}. A: original Fe/ZSM-5(20). B: A calcined at 700 °C. C: A steamed at 700 °C.

an almost four times over-exchange compared with an ordinary ion-exchange method [3].

The proposal of the reaction [4,5]

$$\text{Z-OH} + FeCl_3 \longrightarrow [\text{Z-O}]^-[FeCl_2]^+ + HCl\uparrow \quad (1)$$

explains a three-fold higher exchange compared with ion exchange. However, in the gas phase, molecular $FeCl_3$ exists in the binuclear form of Fe_2Cl_6 that has a puckered four-membered Fe_2Cl_2 ring [23]. In a relatively Al-rich zeolite, the reaction may proceed as

$$2\,\text{Z-OH} + Fe_2Cl_6 \longrightarrow 2[\text{Z-O}]^-[Fe_2Cl_4]^{2+} + 2HCl\uparrow \quad (2)$$

However, for a high Si/Al ratio, the concentration of vicinal protons is low and part of the reaction can be described as

$$\text{Z-OH} + Fe_2Cl_6 \longrightarrow [\text{Z-O}]^-[Fe_2Cl_5]^+ + HCl\uparrow \quad (3)$$

This reaction provides a way of introducing two Fe^{3+} for one proton into the zeolite. Consequently, Fe/ZSM-5(30) has a similar Fe content loading as Fe/ZSM-5(20). As pointed out by Dědeček *et al.* [24], the Al distribution in silicon-rich zeolite is not random but depends on the chemical composition and the condition of synthesis. This may lead to three or even fewer chlorine atoms in the adsorbed iron complex.

3.2. Catalytic performance

Figures 1 and 2 show the relation between the temperature and conversion of the N_2O decomposition over Fe/ZSM-5(20) and Fe/ZSM-5(30), respectively. N_2O decomposes to N_2 and O_2 stoichiometrically and neither NO nor NO_2 is detected.

As can be seen from figure 1, the conversion increases with the increase of temperature. For the original Fe/ZSM-5(20), the conversion reaches 100% at 500 °C. Further treatment (high-temperature calcination or steaming) increases the catalytic activity. For the steamed Fe/ZSM-5(20), the N_2O decomposition starts at around 350 °C and 100% conversion has been found at 450 °C. The efficiency of the high-temperature calcined Fe/ZSM-5(20) is a little lower than that of the steamed Fe/ZSM-5(20). Similar trends are observed for the various Fe/ZSM-5(30). However, Fe/ZSM-5(30) exhibits lower activity compared to Fe/ZSM-5(20) although they have the similar Fe content, possibly due to lower number of active sites.

3.3. Arrhenius plot

The rate of N_2O decomposition can be written as

$$r = kP^n_{N_2O} = A\,e^{-(E_a/RT)}P^n_{N_2O} \quad (4)$$

Our results (not shown) and other investigators' results [21,25] indicate that the N_2O decomposition is a first-order reaction ($n = 1$). Arrhenius plots for the N_2O decomposition over Fe/ZSM-5(20) and Fe/ZSM-5(30) are shown in figures 3 and 4, respectively. The apparent activation energies and $\ln A$ (apparent pre-exponential factor) for various catalysts are shown in table 2.

Table 2 shows that the apparent activation energy of the original Fe/ZSM-5 catalyst is in the range 136–151 kJ/mol, depending on Si/Al ratio. After high-temperature calcination or steaming, the apparent activation energies increase to around 200 kJ/mol. Simultaneously, the apparent pre-exponential factor increases in the order of $\sim 10^4$–10^5. The higher activity is thus explained by the compensation effect, resulting in an increase of the pre-exponential factor.

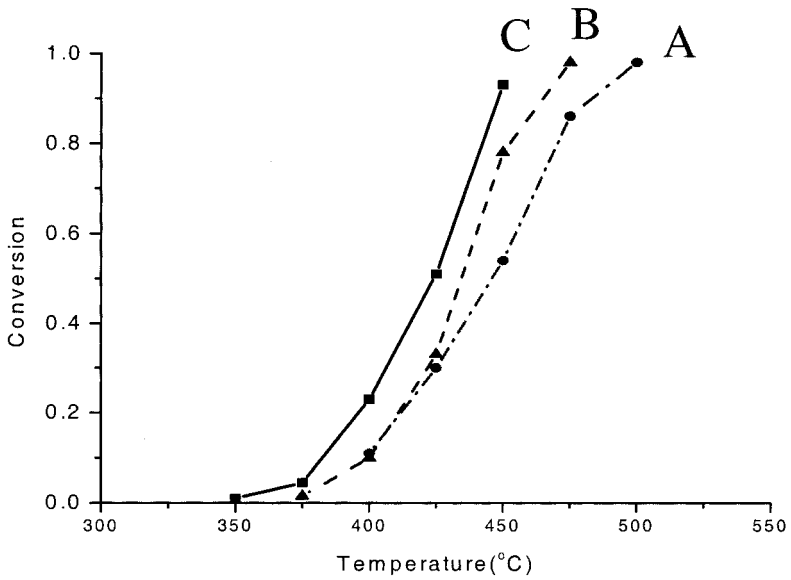

Figure 2. N_2O decomposition on Fe/ZSM-5(30). Feed concentration: 3500 ppm GHSV = 24 000 h^{-1}. A: original Fe/ZSM-5(30). B: A calcined at 700 °C. C: A steamed at 700 °C.

3.4. Characterization

3.4.1. IR

Figure 5 shows the infrared spectra for the various Fe/ZSM-5(20) catalysts, including the parent HZSM-5. The band at 3613 cm^{-1} is the stretching vibration of the Brønsted hydroxyl groups, while the band at 3745 cm^{-1} relates to the vibrations of terminal Si–OH groups [26,27]. Generally, the band at 3665 cm^{-1} is assigned to the hydroxyl groups connected to extra-lattice aluminum [28]. By calibration with the overtone of the lattice vibrations, we were able to calculate the amount of hydroxyl groups.

Chen and Sachtler [4] found the disappearance of Brønsted acidity after sublimation of the $FeCl_3$ complex. The data for the original Fe/ZSM-5(20) (figure 5, trace B) clearly indicate that some of the Brønsted acidity (approximately 45%) is regenerated after washing and calcination at 550 °C. The remaining charge-compensation derives from the coordination of cationic Fe species to the zeolite.

After calcination at 700 °C (figure 5, trace C), the band at 3613 cm^{-1} is lower and we calculate that approximately 8% of the original Brønsted acid sites persist. A similar effect is found after steaming (figure 5, trace D). In this case, a small increase in the band at 3665 cm^{-1} might point to partial dealumination of the zeolite structure. XRD spectra of the various samples showed that the MFI structure remains intact, while the steaming treatment results in a small increase of the amorphous phase.

3.4.2. NMR

Figure 6 shows the magic-angle spinning (MAS) ^{27}Al NMR spectra of Fe/ZSM-5(20) at a sample rotation rate of 12.5 kHz. Intense MAS sidebands (indicated by $*$) are observed as compared with the MAS ^{27}Al NMR spectrum of the parent zeolite HZSM-5 (not shown). This is a result of the strong dipolar interaction between the ^{27}Al nuclei and the paramagnetic Fe^{3+} ions. The

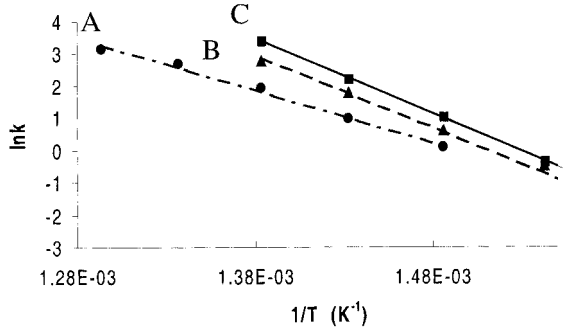

Figure 3. Arrhenius plot of N_2O decomposition on Fe/ZSM-5(20). A: original Fe/ZSM-5(20). B: A calcined at 700 °C. C: A steamed at 700 °C.

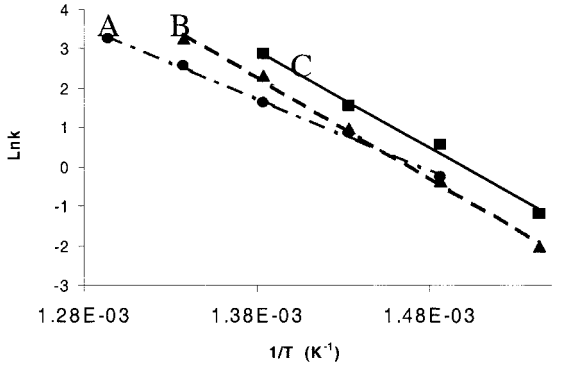

Figure 4. Arrhenius plot of N_2O decomposition on Fe/ZSM-5(30). A: original Fe/ZSM-5(30). B: A calcined at 700 °C. C: A steamed at 700 °C.

Table 2
Kinetic parameters of the reaction

	Original		High-temperature calcined		Steamed	
	Fe/ZSM-5(20)	Fe/ZSM-5(30)	Fe/ZSM-5(20)	Fe/ZSM-5(30)	Fe/ZSM-5(20)	Fe/ZSM-5(30)
Ln A (A: s^{-1})	24.5	26.8	33.8	37.7	35.8	37.1
E_a (kJ/mol)	136	151	186	213	195	205

band pattern centered on 56 ppm is assigned to the tetrahedrally coordinated Al in the zeolite lattice. The weak band at 0 ppm belongs to a small fraction of octahedrally-coordinated extra-lattice Al. This is consistent with the findings of a signal of hydroxyl groups associated with extra-lattice Al at 3665 cm^{-1} (figure 5, trace B). After high-temperature calcination (figure 6, trace B), no obvious change is observed except that the total intensity is reduced drastically. However, after steaming, a new broad peak is detected at 37 ppm. Typically, this peak is attributed to non-lattice tetrahedrally- or pentahedrally-coordinated aluminum [29]. Such Al may exist in the MFI micropores as the Al_2O_3 without associated hydroxyl group and this might explain why we cannot detect the increase of the 3665 cm^{-1} in the steamed Fe/ZSM-5(20) (figure 5, trace D). Apparently, such extra-lattice aluminum is produced by steaming. We estimate that about 10% lattice aluminum is dislodged from the lattice that also contributes to the disappearance of Brønsted acid. On the contrary, the absence of a peak around 37 ppm for the high-temperature calcined Fe/ZSM-5(20) (figure 6, trace B) also indicates that the disappearance of Brønsted acidity must originate from the reaction of the protons with Fe species at 700 °C.

3.4.3. ESR

Since the ferric iron, with unpaired electrons in the 3d shell, is paramagnetic in both the low-spin and high-spin electronic configurations, ESR spectroscopy is a powerful and sensitive method to characterize the Fe species, although the assignment and identification of Fe species by this technique is by no means conclusive [30,31].

The ESR spectra of all Fe/ZSM-5(20) samples, recorded at 10 K are reported in figure 7. The spectra at this temperature show a better resolution of the overlapping lines than the spectra at room temperature (not shown). The original Fe/ZSM-5(20) shows signals at $g = 4.4$, $g = 5.7$ and $g = 6.6$ with a broad line in the low field. At high field, a broad line centered at $g = 2.1$ is obvious with a shoulder at $g = 2.0$. These signals have been reported in the literature [21,26,31,32], but the assignment to various Fe species is not unequivocal. In general, the signal at $g = 4.4$ is assigned to isolated tetrahedrally-coordinated Fe that has a strong rhombic distortion, while the $g = 5.7$ and $g = 6.6$ signals are assigned to strongly axially-distorted tetrahedrally-coordinated Fe species [33]. It is worth pointing out that the narrow line of $g = 4.4$ cannot be used to exclusively confirm the presence of Fe^{3+} in the zeolite

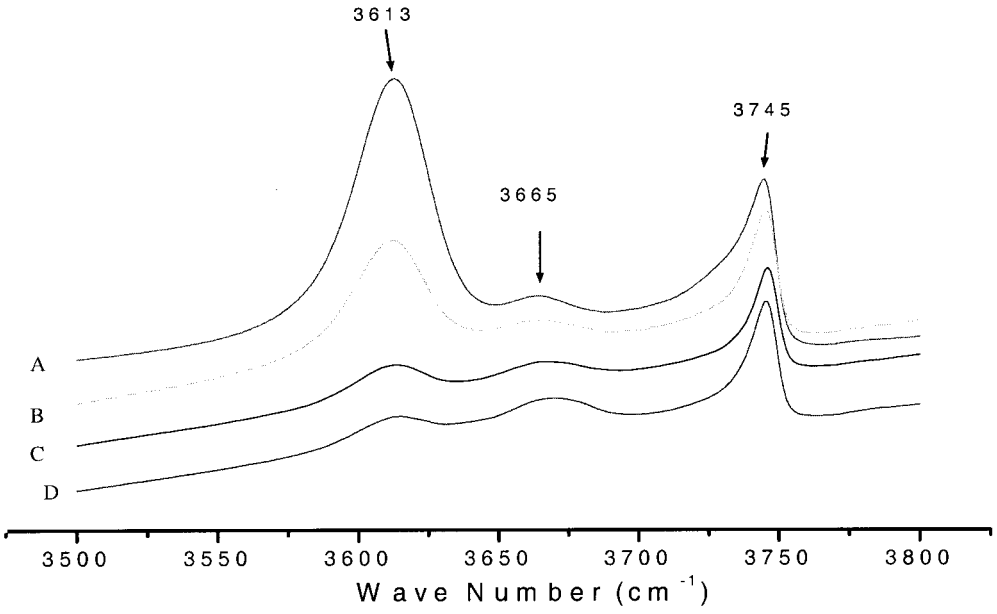

Figure 5. IR spectra of the parent HZSM-5(20) and Fe/ZSM-5(20). A: parent HZSM-5(20). B: original Fe/ZSM-5(20). C: B calcined at 700 °C. D: B steamed at 700 °C.

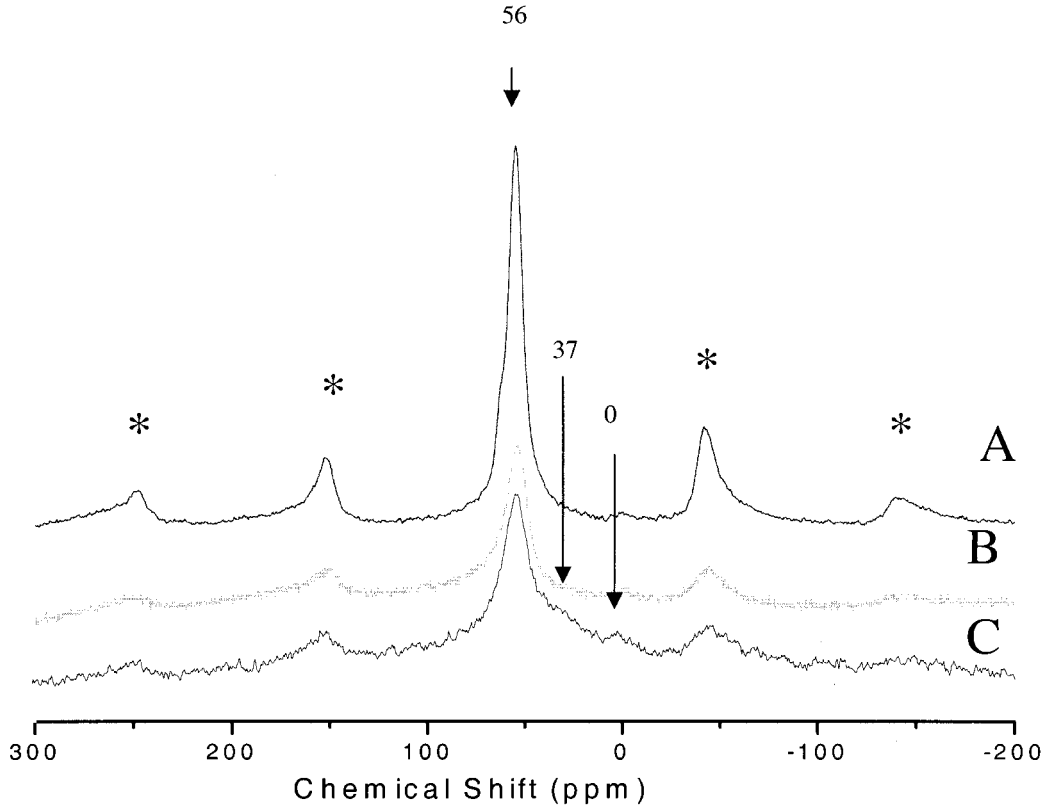

Figure 6. ^{27}Al MAS NMR spectra of Fe/ZSM-5(20). A: original Fe/ZSM-5(20). B: A calcined at 700 °C. C: A steamed at 700 °C.

lattice positions [30]. We propose that part of the signal $g = 4.4$ is due to the mononuclear $(Fe{=}O)^{+}$ that is strongly distorted by the negative charge of vicinal framework Al [34]. Generally, the signals at $g = 5.7$ and $g = 6.6$ are assigned to isolated Fe^{3+} cations in distorted tetrahedral coordination [32]. The weak signal at 2.0 is generally attributed to octahedral Fe^{3+} in the cationic position of the zeolite [21,26]. The various

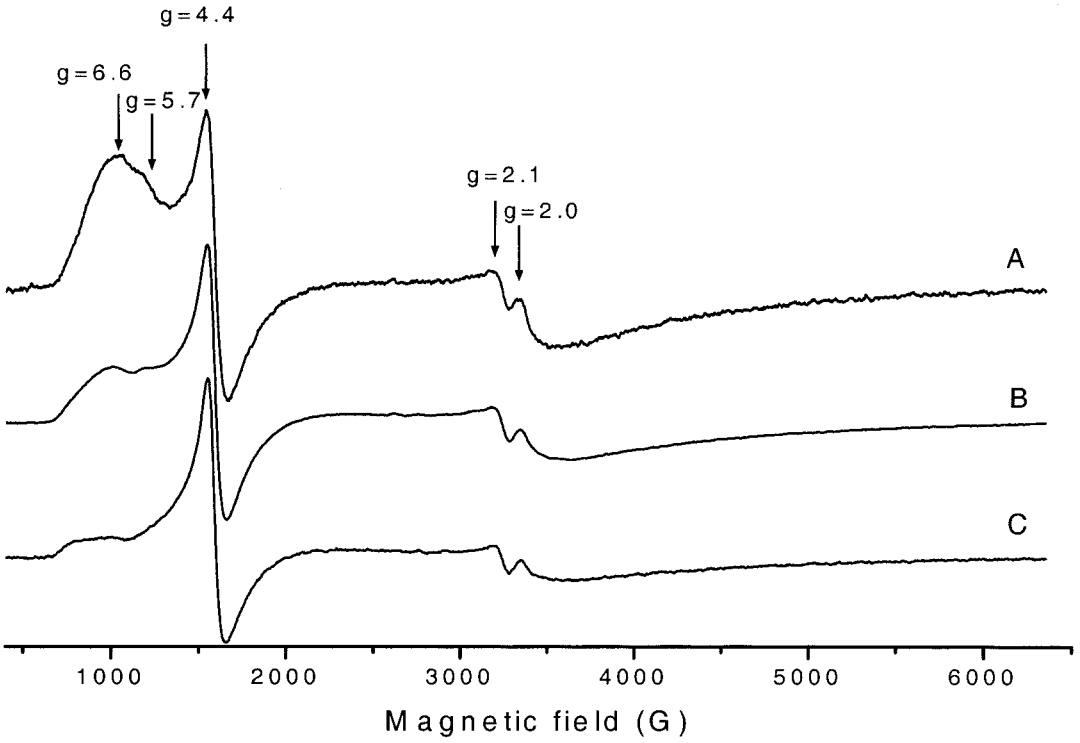

Figure 7. ESR spectra of Fe/ZSM-5(20), measured at 10 K. A: original Fe/ZSM-5(20). B: A calcined at 700 °C. C: A steamed at 700 °C.

spectra indicate a signal at $g = 2.1$ that we assign to an agglomerate of iron oxide on the external zeolite surface. Further treatments of the original Fe/ZSM-5(20) cause some changes in the ESR spectra. Most significantly, the signals at $g = 5.7/6.6$ drastically decrease for both the calcination and the steaming treatment. It is worth pointing out that in the ESR spectra of Fe/ZSM-5(30) (not shown), we also observe a similar decrease of the signals at $g = 5.7/6.6$ and an increase of the signal $g = 4.4$, when applying the same amount of the various samples.

4. Discussion

The first over-exchanged Fe/ZSM-5 [2,3], a highly-durable promising catalyst in the selective catalytic reduction of NO_x, proved later to be difficult to reproduce [27,35], possibly due to the different synthesis method of the parent zeolite [35]. The sublimation of $FeCl_3$ on HZSM-5 provides an alternative method to achieve over-exchanged Fe/ZSM-5. However, in this preparation method, almost every step influences the final distribution of the Fe species in the zeolite. Maturano *et al.* [15] concluded that formation of various Fe species is related to the washing procedure after sublimation while Battiston (personal communication) proposed that calcination is a crucial step in the final distribution of Fe species. Furthermore, in our preparation, we found that the formation of iron oxide can be partly suppressed (not shown) by adjusting the pressure of $FeCl_3$ vapor in the sublimation procedure. Thus, it can be concluded that the preparation of over-exchanged Fe/ZSM-5 is a very subtle art.

During the sublimation procedure, all the protons of the parent HZSM-5 are replaced by iron-chlorine complexes [4]. After washing, drying and calcination, part of the Brønsted acid sites (45%) are regenerated, proving indirectly the formation of iron oxy–hydroxide species instead of naked Fe^{3+} cations. Evidently, ESR indicates the presence of a variety of Fe species in the over-exchanged Fe/ZSM-5. The sum of the regenerated Brønsted acid sites and the iron-containing cations (including naked Fe^{3+} cation) are used to counterbalance the negative charge of the framework. The hydrolysis of the Fe–chlorine complex in the washing step and calcination step results in neutral Fe oxide presented as bulky iron agglomerates on the external surface, neutral nanoclusters in the micropores and positively charged Fe^{3+} species, possibly binuclear Fe species as proposed by Sachtler [7]. Note that after high-temperature calcination or steaming treatment, nearly 90% of the Brønsted acid sites disappear. Thus, we conclude that Fe-containing cationic species are the main components. The disappearance of Brønsted acidity during the steaming treatment can only be partially attributed to dealumination, as pointed out by IR and NMR. For the high-temperature calcination, we did not observe dealumination, while again a strong decrease in Brønsted acidity was found. Thus, we conclude that further treatment of original Fe-ZSM-5 could lead to the reaction of Fe species with the zeolite protons.

We propose the following mechanism:

$$\mathrm{Fe}_x\mathrm{O}_y + \mathrm{H}^+ \xrightarrow{700\,^\circ\mathrm{C}} (\mathrm{FeO})^+ + \mathrm{H_2O} \qquad (5)$$

$\downarrow$ 3613 cm^{-1} in IR

$\downarrow$ strongly rhombically distorted $g = 4.4$

The important point to be made is that some neutral Fe species are converted to cationic species in the zeolite. Neutral species include Fe oxide at the external surface and Fe oxide nanoclusters occluded in the zeolite micropores. However, we propose that it is the nanocluster that reacts with the zeolitic protons. This is supported by our experimental data, showing that bulk Fe oxide clusters, prepared by impregnation of $Fe(NO_3)_3$ on a silica support, are not active in N_2O decomposition at 400 °C. Further evidence is provided by the report that the Fe oxide agglomerate formed by steaming Fe-substituted ZSM-5 on the external surface cannot activate N_2O as oxidant in oxidation of aromatics [31]. Since large Fe oxide clusters are inactive in N_2O decomposition at this temperature, the activity in original Fe/ZSM-5 derives from both Fe oxide nanoclusters and cationic Fe species. The activity is strongly enhanced due to an increase of the cationic Fe species. The almost complete disappearance of Brønsted acidity may indicate that such further treatment leads to a catalyst with almost exclusively cationic Fe species present next to inactive large Fe oxide clusters. The large change in apparent activation energy between original Fe/ZSM-5 and further treated Fe/ZSM-5 as determined over a wide temperature range indicates that indeed the catalytic nature of these species is very different. This is taken as further evidence that the neutral nanoclusters are also able to catalyze N_2O decomposition although at a much lower rate. The much higher apparent activation energy for the more active catalyst is compensated by a high pre-exponential factor. The difference is 4–5 orders of magnitude. Thus, we draw the main conclusion that in Fe/ZSM-5 different Fe species are responsible for N_2O decomposition.

Kapteijn [36] outlined the following elementary steps for N_2O decomposition over Fe/ZSM-5:

Step 1

$$\mathrm{N_2O} + * \xrightarrow{k_1} \mathrm{N_2} + \mathrm{O}^*$$

Step 2

$$2\mathrm{O}^* \underset{k_2}{\overset{k_2}{\rightleftarrows}} \mathrm{O_2}$$

Step 3

$$N_2O + O^* \xrightarrow{k_3} N_2 + O_2 + *$$

The first step is actually a combination of the adsorption of N_2O on the active site and the subsequent deposition of one oxygen atom. Generally, it is found that there is no dependency on oxygen partial pressure, allowing one to neglect the reverse step 2. Our experiments indicate that the surface is fully covered with oxygen species. This indicates that step 3 is a rate-limiting step, leading to

$$r = 2k_3 P_{N_2O} \quad (6)$$

This general expression complies with the observation of first-order dependency in N_2O partial pressure and the absence of an influence of oxygen partial pressure for our set of Fe/ZSM-5 catalysts. In the rate-limiting step 3, adsorbed oxygen reacts with gas phase N_2O. The large change in kinetic parameters can thus be explained by the nature of the adsorbed oxygen atom (O^*). From its higher apparent activation energy, we conclude that the Fe–O^* bond energy is higher for the more active catalyst. Such a strong Fe–O^* bond also leads to a large gain in entropy in the rate-limiting step, providing a tentative explanation for the increase of the pre-exponential factor. The difference in the nature of the Fe species can partly be proven by their oxidation ability towards hydrocarbons. We have done some preliminary tests of the conversion of benzene to phenol using N_2O as the oxidant on various Fe/ZSM-5 samples. In our initial qualitative analysis, the original Fe/ZSM-5 has a very low activity whereas the high-temperature calcined and steamed Fe/ZSM-5 show good catalytic performance.

5. Conclusions

High-temperature treatment of Fe/ZSM-5 prepared by the sublimation method of $FeCl_3$ is found to strongly increase the rate of N_2O decomposition. The activity strongly depends on the nature of Fe species inside the zeolite micropores. In the untreated Fe/ZSM-5 the catalytic activity mainly derives from Fe oxide nanoclusters. Calcination or steaming treatments at 700 °C induce a reaction between these nanoclusters and zeolite protons, resulting in cationic Fe species. Such species have an appreciably higher activity, and kinetic parameters point to a stronger Fe–O bond in this case.

Acknowledgments

The Dutch National Research School Combination Catalysis is gratefully acknowledged for financial support. The authors also thank Dr. A.L. Yakolev and Prof. Zhidomirov for helpful discussions.

References

[1] P.M.M. Blauwhoff, J.W. Gosselink, E.P. Kieffer, S.T. Sie and W.H.J. Stork, in: *Catalysis and Zeolites: Fundamentals and Applications*, eds. J. Weitkamp and L. Puppe (Springer, Berlin, 1999) ch. 7.
[2] X. Feng and W.K. Hall, Catal. Lett. 41 (1996) 45.
[3] X. Feng and W.K. Hall, J. Catal. 166 (1997) 368.
[4] H.-Y. Chen and W.M.H. Sachtler, Catal. Today 42 (1998) 73.
[5] H.-Y. Chen and W.M.H. Sachtler, Catal. Lett. 50 (1998) 125.
[6] H.-Y. Chen, T.V. Voskoboinikov and W.M.H. Sachtler, J. Catal. 180 (1998) 171.
[7] T.V. Voskoboinikov, H.-Y. Chen and W.M.H. Sachtler, Appl. Catal. B 19 (1998) 279.
[8] Q. Sun, Z.-X. Gao, H.-Y. Chen and W.M.H. Sachtler, J. Catal. 201 (1998) 89.
[9] G.I. Panov, V.I. Sobolev and A.S. Kharitonov, J. Mol. Catal. 61 (1990) 85.
[10] V.I. Sobolev, G.I. Panov, A.S. Kharitonov, V.N. Romannikov, A.M. Volodin and K.G. Ione, J. Catal. 139 (1993) 435.
[11] V.I. Sobolev, K.A. Dubkov, E.A. Paukshtis, L.V. Pirutko, M.A. Rodkin, A.S. Kharitonov and G.I. Panov, Appl. Catal A. 141 (1996) 185.
[12] G.I. Panov, V.I. Sobolev, K.A. Dubkov,V.N. Parmon, N.S. Ovanesyan, A.E. Shilov and A.A. Shteinman, React. Kinet. Catal. Lett. 61 (1997) 251.
[13] K.A. Dubkov, V.I. Sobolev, E.P. Talsi, M.A. Rodkin, N.H. Watkins, A.A. Shteinman and G.I. Panov, J. Mol. Catal. 123 (1997) 155.
[14] G.I. Panov, V.I. Sobolev, K.A. Dubkov and A.S. Kharitonov, Stud. Surf. Sci. Catal. 101 (1996) 493.
[15] P. Marturano, L. Drozdová, A. Kogelbauer and R. Prins, J. Catal. 192 (2000) 236.
[16] A.A. Battiston, J.H. Bitter and D.C. Koningsberger, Catal. Lett. 66 (2000) 75.
[17] H.-Y. Chen, El-M. El-Malki, X. Wang, R.A. van Santen and W.M.H. Sachtler, J. Mol. Catal. 162 (2000) 159.
[18] R. Joyner and M. Stockenhuber, J. Phys. Chem. B. 103 (1999) 5963.
[19] L.J. Lobree, I.-C. Hwang, J.A. Reimer and A.T. Bell, J. Catal. 186 (1999) 242.
[20] El-M. El-Malki, R.A. van Santen and W.M.H. Sachtler, Microporous Mesoporous Mater. 35–36 (2000) 235.
[21] El-M. El-Malki, R.A. van Santen and W.M.H. Sachtler, J. Catal. 196 (2000) 212.
[22] G. Centi and F. Vazzana, Catal. Today 53 (1998) 683.
[23] F.A. Cotton, G. Wilkinson, C.A. Murillo and M. Bochmam, in: *Advanced Inorganic Chemistry* (Wiley, New York, 1999) p. 778.
[24] J. Dědeček, D. Kaucký and B. Wichterlová. Chem. Commun. 11 (2001) 970.
[25] F. Kapteijn, J. Rodríguez-Mirasol and J.A. Moulijn, J. Catal. 167 (1997) 256.
[26] El-M. El-Malki, R.A. van Santen and W.M.H. Sachtler, J. Phys. Chem. B 103 (1999) 4611.
[27] P. Marturano, A. Kogelbauer and R. Prins, J. Catal. 190 (2000) 460.
[28] P.O. Fritz and J.H. Lunsford, J. Catal. 118 (1989) 85.
[29] J.L. Motz, H. Heinichen and W.F. Hölderich, J. Mol. Catal. 136 (1998) 175.
[30] D. Goldfarb, M. Bernardo, K.G. Strohmaier, D.E.W. Vaughan and H. Thomann, J. Am. Chem. Soc. 116 (1994) 6344.
[31] A. Ribera, I.W.C.E. Arends, S. de Vries, J. Pérez-Ramírez and R.A. Sheldon, J. Catal. 195 (2000) 287.
[32] A.V. Kucherov, C.N. Montreuil, T.N. Kucherova and M. Shelf, Catal. Lett. 56 (1998) 173.
[33] B. Angelika, in: *Spectroscopy of Transition Metal Ions on Surfaces*, eds. B.M. Weckhuysen, P. Van Der Voort and G. Catana (Leuven University Press, Leuven, 1990), p. 69.
[34] A.M. Volodin, V.I. Sobolev and G.M. Zhidomirov, Kinet. Catal. 39 (1998) 844.
[35] X. Feng and W.K. Hall, Catal. Lett. 52 (1997) 13.
[36] F. Kapteijn, J. Rodríguez-Mirasol and J.A. Moulijn, Appl. Catal. B 9 (1996) 25.